ACADEMIC PRESS

Available online at www.sciencedirect.com
SCIENCE DIRECT®

Journal of Catalysis 217 (2003) 30–37

JOURNAL OF CATALYSIS

www.elsevier.com/locate/jcat

Tungsten oxide catalysts supported on activated carbons: effect of tungsten precursor and pretreatment on dispersion, distribution, and surface acidity of catalysts

A.F. Pérez-Cadenas,[a] C. Moreno-Castilla,[a,*] F.J. Maldonado-Hódar,[a] and J.L.G. Fierro [b]

[a] *Departamento de Química Inorgánica, Facultad de Ciencias, Universidad de Granada, 18071, Granada, Spain*
[b] *Instituto de Catálisis y Petroleoquímica, CSIC, Cantoblanco, 28049, Madrid, Spain*

Received 31 July 2002; revised 24 January 2003; accepted 7 February 2003

Abstract

Tungsten catalysts supported on activated carbon were prepared using tungsten hexacarbonyl, ammonium tungstate, and tungsten pentaethoxide. The catalysts were pretreated in He, dry air, or wet air at 623 K for 6 h before being characterized by N_2 adsorption at 77 K, temperature-programmed desorption, X-ray diffraction, high-resolution transmission electron microscopy, and X-ray photoelectron spectroscopy, and by testing their behavior in the decomposition reaction of isopropanol. The dispersion of the supported tungsten oxide phase and their surface acidity depended on the metal precursor and atmosphere of pretreatments. Thus, the highest dispersion and surface acidity were found for the catalyst prepared from $W(CO)_6$ and the lowest dispersion for that prepared from $(NH_4)_2WO_4$. Dry air gave the highest dispersion, whereas wet air yielded the highest surface acidity. Air pretreatments of the catalyst prepared from $W(CO)_6$ seem to create metal oxide–support interactions, because of the very low particle size of the supported tungsten oxide phase and its homogeneous distribution.

Keywords: Tungsten oxide catalysts; Carbon support; Total surface acidity

1. Introduction

Tungsten oxide is a solid of acidic character with many applications in heterogeneous catalysis. There has been wide study of this catalyst supported on different materials [1–27] but scant investigation of its use supported on carbon [28–34], despite the importance of carbon as a support [35]. We previously described the influence of both the tungsten oxide content of the carbon-supported catalyst and the temperature of treatment in inert atmosphere (He) on its textural properties, chemical composition, dispersion, and surface acidity [30], and on its behavior in the skeletal isomerization of 1-butene [29,31] and the dehydration of alcohols [32]. We found that pretreatment in He at 623 K produced the catalysts with highest surface acidity and, therefore, with greatest activity in the isomerization of 1-butene. Following this line of research, the present work studied the effect of the tungsten precursor used and of the nature of the pretreatment atmosphere on the dispersion, distribution, and surface acidity of supported tungsten oxide. For this purpose, tungsten oxide was deposited on activated carbon obtained from olive stones, using the following precursors: tungsten hexacarbonyl, ammonium tungstate, and tungsten pentaethoxide. The catalysts so prepared were pretreated at 623 K for 6 h in He, dry air, or wet air before being characterized by different techniques.

2. Experimental

The activated carbon used as support was obtained from olive stones. Previously, they were ground and sieved to obtain a particle size between 1.4 and 2.4 mm. They were then carbonized in N_2 flow at 1123 K for 15 min and activated in CO_2 flow at 1123 K for 4 h, as described in detail elsewhere [36]. The burn-off of the carbonized sample during its activation was 22%. The activated carbon thus obtained was sieved again and the particle size between 1

* Corresponding author.
E-mail address: cmoreno@ugr.es (C. Moreno-Castilla).

0021-9517/03/$ – see front matter
doi:10.1016/S0021-9517(03)00059-9

Table 1
Tungsten content of the different supported catalysts

Sample	% *W*
HW	8.0
HWa	7.4
HWe	6.9

and 2 mm was used. This sample, with an ash content of 0.4%, will be referred to hereafter as H.

The catalysts were prepared from three different precursors: tungsten hexacarbonyl, ammonium tungstate, and tungsten pentaethoxide. A previously described sublimation technique [37,38] was used for $W(CO)_6$. The preparation of the catalyst from $(NH_4)_2WO_4$ was by impregnation of the support with an aqueous solution of the above salt, as described in detail elsewhere [30]. Finally, the preparation of the catalyst from $W(OEt)_5$ was carried out by adsorption from an *n*-hexane solution of the alkoxide. For this purpose, the activated carbon was outgassed under vacuum at room temperature for 1 h. The appropriate amount of alkoxide was then dissolved in the minimum amount of *n*-hexane required to cover the activated carbon and was injected through a septum in the flask containing the support. After 12 h of contact time, the residue of the solvent was eliminated in N_2 flow at room temperature. Finally, the catalyst was dried overnight at 383 K.

The prepared catalysts will be referred to hereafter as HW, HWa, and HWe, corresponding to the use of precursors $W(CO)_6$, $(NH_4)_2WO_4$, and $W(OEt)_5$, respectively.

The exact tungsten content of the supported catalyst was determined in a thermobalance by burning a portion of the catalyst in a flow of air at 1273 K until constant weight. The tungsten content of the catalysts is given in Table 1.

Before the catalysts were characterized, they were heated in He or dry or wet air at 623 K for 6 h. Wet air was obtained by saturation of an air flow with water at 298 K. Once the treatment was finished, the samples were cooled to the desired temperature in the same flow except in the case of the samples treated in wet air, which was changed to dry air.

Characterization of the supported catalysts was carried out by the following methods: N_2 adsorption at 77 K, from which the micropore volume applying the DR equation [39] and the BET surface area were obtained; temperature-programmed desorption (TPD); X-ray diffraction (XRD); high-resolution transmission electron microscopy (HRTEM); X-ray photoelectron spectroscopy (XPS); and measurement of surface acidity from the decomposition reaction of isopropanol.

TPD was carried out by heating the samples at different temperatures up to a maximum of 1273 K in He flow (60 $cm^3\,min^{-1}$) at a heating rate of 50 $K\,min^{-1}$. The amount of evolved gases was recorded as a function of temperature using a quadrupole mass spectrometer (Balzers, Model Thermocube), as described elsewhere [30].

XRD patterns were recorded with a Phillips PW1710 diffractometer using Cu-K_α radiation. JCPDS files were searched to assign the different diffraction peaks observed.

HRTEM was carried out with a Phillips electron microscope, Model CM-20, equipment that used an EDAX microanalysis system. Magnification was 600,000×, and maximum resolution was 0.27 nm between points and 0.14 nm between lines.

XPS measurements were made with an Escalab 200R system (VG Scientific Co.) equipped with Mg-K_α X-ray source ($h\gamma = 1253.6$ eV) and hemispherical electron analyzer. Prior to the analysis, the samples were pretreated in situ at 623 K for 6 h in He, dry air, or wet air. Once the treatment was finished, the samples were cooled to the desired temperature in the same flow, except in the case of the samples treated in wet air, which was changed to dry air. They were then evacuated at high vacuum and introduced into the analysis chamber. A base pressure of 10^{-9} mbar was maintained during data acquisition. Survey and multiregion spectra were recorded at C_{1S}, O_{1S}, and W_{4f} photoelectron peaks. Each spectral region of photoelectron interest was scanned several times to obtain good signal-to-noise ratios. The spectra obtained after background signal correction were fitted to Lorentzian and Gaussian curves in order to obtain the number of components, the position of the peak, and the peak areas.

Surface acidity of the supported catalysts was evaluated by studying the decomposition reactions of isopropanol, using a plug-flow microreactor working at atmospheric pressure with He as carrier gas. The experimental procedure is described in detail elsewhere [40]. Prior to the catalytic activity measurements, the samples were pretreated at 623 K for 6 h in He, dry air, or wet air.

Analysis of the reaction products was carried out by online gas chromatography. Propene and acetone were the main reaction products obtained. Very small amounts of diisopropylether were also detected in all cases. The activity to obtain a given species, r_x, was calculated using

$$r_x = \frac{F_{\mathrm{Iso}} \cdot C_x}{W}, \tag{1}$$

where F_{Iso} is the isopropanol flow through the catalyst in moles per min, C_x is the isopropanol conversion to species x, and W is the weight (g) of tungsten in the supported catalyst. The reaction was carried out in the temperature range between 343 and 393 K. Apparent activation energy was obtained by applying the Arrhenius equation to the activity data obtained at different temperatures.

3. Results and discussion

Table 2 shows the micropore volume (W_0) and nitrogen surface area (S_{N_2}) of the support, H, and of some of the supported catalysts after different pretreatments. For the support, the volumes of mesopores with pore width between

Table 2
BET surface area of the support and the supported catalysts after different pretreatments at 623 K for 6 h

Sample	Pretreatment	W_0 ($cm^3\,g^{-1}$)	S_{N_2} ($m^2\,g^{-1}$)
H	–	0.29	691
HW	He	0.23	579
HW	Dry air	0.25	636
HW	Wet air	0.27	673
HWa	Wet air	0.26	631
HWe	Wet air	0.24	607

3.7 and 50 nm and macropores (pore width > 50 nm) were obtained from mercury porosimetry. The values of these pore volumes were 0.13 and 0.79 cm^3/g, respectively. Therefore, the support had a more developed macroporosity compared with its meso- or microporosity. The external surface area value was 55 m^2/g, much lower than the nitrogen surface area value. W_0 and S_{N_2} of the supported catalysts depended on the pretreatment and on the precursor used in their preparation. Thus, in the HW catalysts, both parameters increased in the order He < dry air < wet air and, after this last pretreatment, showed fairly similar values to those of the support. Treatments in oxidant atmospheres may favor a slight gasification of the support catalyzed by the tungsten oxide produced during the pretreatment.

After the wet air pretreatment both W_0 and S_{N_2} slightly decreased in the order HW > HWa > HWe, which may be related to the dispersion and distribution of the metal oxide. This is because the pore model in activated carbons consists of an interconnected network of pores of different sizes: micro-, meso-, and macropores. Gas molecules can only reach microporosity by passing through meso- and macropores [41]. However, when large metal oxide crystallites are deposited on an activated carbon there is the possibility of blocking the entrance of large pores, which would also block the access to a portion of smaller pores. Therefore, the greater the particle size of the tungsten oxide, the more micropores are blocked, and the lower the surface area.

All catalysts were analyzed by XRD after their respective pretreatments and no diffraction peaks were found in their patterns. This indicates that the tungsten oxide obtained during the pretreatment either has a particle size below 4 nm or is formed by very thin particles with low crystallinity.

Catalysts were also analyzed by HRTEM after some of the pretreatments. No metal oxide particles were observed in the HW catalyst pretreated in wet air, implying that the metal oxide had a very high dispersion or was formed by very thin sheets. In contrast, metal oxide particles were observed in the other catalysts studied and a small number of them showed electron diffraction patterns (Fig. 1). This pattern only appeared in some directions and disappeared when the particles were twisted. This may indicate that the metal oxide particles were very thin sheets or films. Fig. 2 shows the crystallographic planes of a metal oxide particle from catalyst HWa pretreated in wet air. The distance between planes was calculated from Fig. 2 to be $d_{hkl} = 0.386$ nm,

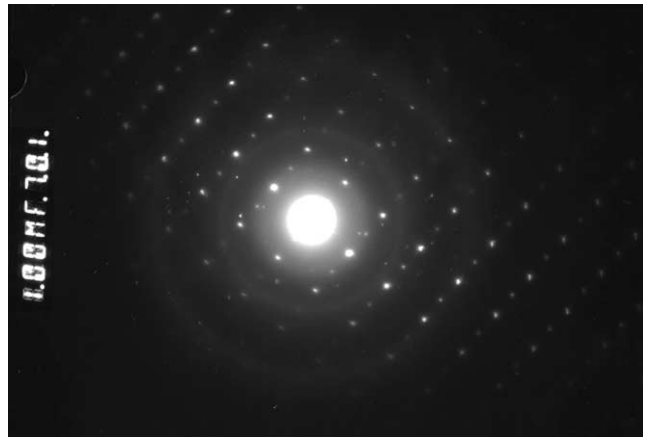

Fig. 1. Electron diffraction pattern of a tungsten oxide nanoparticle from catalyst HWa pretreated in wet air.

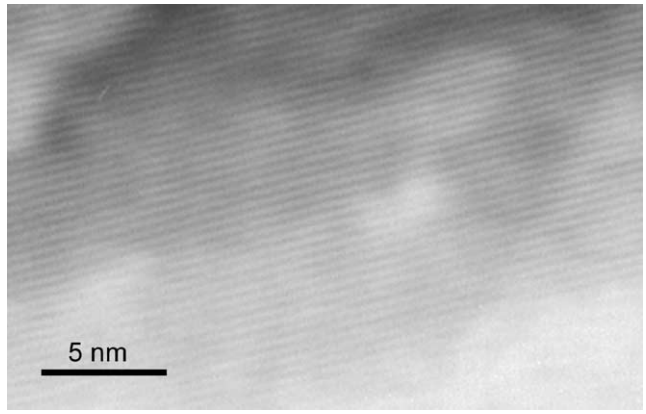

Fig. 2. Lines corresponding to the crystallographic planes of a tungsten oxide nanoparticle from catalyst HWa pretreated in wet air.

Table 3
Mean particle size of tungsten oxide in various supported catalysts obtained by HRTEM

Sample	Pretreatment	d (nm)
HW	Wet air	n.d.[a]
HWe	Wet air	54
HWa	Wet air	111
HWa	He	65

[a] n.d., nondetected.

very close to the d-spacing of (001) planes in tungsten trioxide ($d_{001} = 0.385$ nm, from file JCPDS-20-1324).

The mean crystallite size of the tungsten oxide was calculated from different microphotographs. According to these results, the dispersion of the metal oxide particles follows the order HW ≫ HWe > HWa after wet-air pretreatment (Table 3). The metal oxide particles in HW catalysts must be formed by extremely thin sheets or films, with no crystallinity. In the case of HWa, pretreatment in He yielded a more dispersed catalyst in comparison with pretreatment in wet air, which may be because humidity favors the sintering of the metal oxide particles.

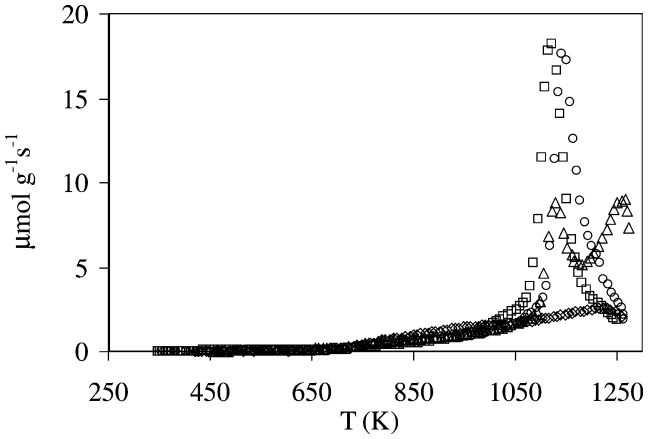

Fig. 3. CO desorption profiles from samples H (◇), HWa (△), HW (□), and HWe (○) pretreated in He.

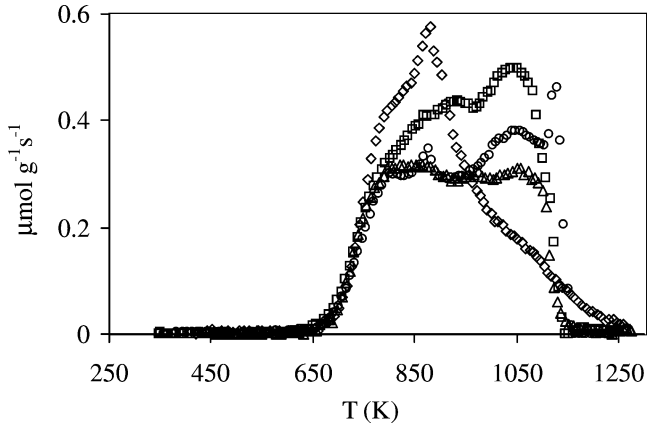

Fig. 4. CO_2 desorption profiles from samples H (◇), HWa (△), HW (□), and HWe (○) pretreated in He.

Figs. 3 and 4 depict the CO and CO_2 desorption profiles, respectively, of the catalysts HW, HWa, and HWe and the support H after pretreatment in He. The amounts of CO and CO_2 desorbed were obtained from these profiles (Table 4). The catalysts showed a CO desorption peak at around 1130 K, with a much greater amount of CO desorbed in comparison with support H. This indicates that the tungsten oxide formed during either the preparation or pretreatment was reduced by the support at the above temperature. This reduction, which was previously reported [30], is thermodynamically favored [42].

The reduction of 1 mol of tungsten trioxide by the support will yield 3 mol of CO. Thus, the amount of CO evolved during the complete reduction of tungsten trioxide was calculated by taking into account the tungsten oxide content of each catalyst. This amount, shown in parentheses in Table 4, was similar to the ΔCO value, which was obtained by subtracting the CO evolved from each catalyst from that evolved from the support.

The amount of CO_2 desorbed from the catalysts was comparable to that evolved from the support, so that the reduction of the tungsten oxide by the support only yielded CO. This result also indicates that the disproportionate reaction of the CO formed, catalyzed by the metal oxide phase, can be ruled out. Therefore, the ΔCO of the catalysts is only due to the reduction of tungsten oxide by the support. This reduction is easier when the metal oxide phase is more dispersed, because of the larger area of contact between the carbon support and the metal oxide particles.

Catalysts HW and HWe showed only one CO desorption peak (at 1130 K), whereas catalyst HWa showed two peaks (at 1130 and 1260 K). This may indicate a greater resistance to the reduction of tungsten oxide in catalyst HWa, because of the presence of larger tungsten oxide particles (lower dispersion).

The amounts of evolved CO and CO_2 after the dry- and wet-air pretreatments of the catalysts and the support were obtained from the respective desorption profiles (Table 4). The amounts of CO desorbed from the catalysts after pretreatments in air were greater than after pretreatment in He. This indicates that oxygen surface complexes that thermally evolve as CO are fixed on the carbon surface during pretreatment in air. Therefore, the amount of CO evolved from the catalysts comes from both the reduction of tungsten oxide by the support and the decomposition of oxygen surface complexes.

Table 4
Amounts of CO and CO_2 (µmol g^{-1}) desorbed to 1273 K from the support and the supported catalysts after different pretreatments

Sample	Pretreatment	CO	ΔCO	CO_2	ΔCO_2	*Q*
H	He	832		164		–
HW	He	2069	1238 (1305)[a]	197	33	–
HWe	He	2047	1215 (1208)	167	3	–
HWa	He	2024	1192 (1126)	142	−22	–
H	Wet air	2429		298		–
HW	Wet air	3701	1272	629	331	1934
HWe	Wet air	3197	768	523	225	1218
HWa	Wet air	2990	561	368	70	700
H	Dry air	2729		372		–
HW	Dry air	4047	1318	840	469	2255
HWe	Dry air	3802	1073	802	431	1934
HWa	Dry air	3257	528	525	153	834

[a] Values in parentheses are the theoretical values for the reduction of tungsten trioxide.

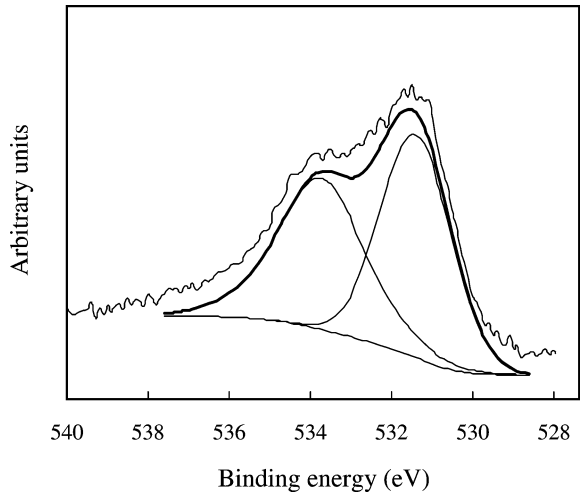

Fig. 5. Curve-fitted O_{1S} core-level spectra for catalyst HW pretreated in wet air.

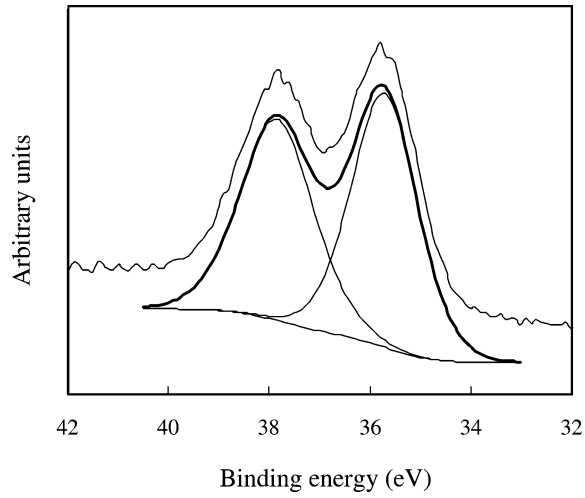

Fig. 6. Curve-fitted W_{4f} core-level spectra for catalyst HW pretreated in wet air.

After the air pretreatments, the amount of CO_2 evolved from the catalysts was greater than that evolved from the support, because of the fixation of oxygen surface complexes on the carbon support during the pretreatments.

The amounts of CO and CO_2 evolved from the catalysts increased because the tungsten particles can dissociatively chemisorb oxygen from the air. The subsequent migration of the oxygen to the support yields oxygen surface complexes at the tungsten oxide–carbon interface that thermally evolve as CO and CO_2. This process directly depends on the dispersion of the metal oxide phase. In addition, the amount of CO desorbed, which derives from the reduction of the tungsten oxide by the support, is also related to the dispersion.

A parameter Q, closely related to the dispersion of the tungsten oxide, can therefore be defined as

$$Q\left(\mu\text{mol}_{\text{Oxygen}}\,\text{g}^{-1}\right) = [\text{CO}_{\text{Cat}} - \text{CO}_{\text{Sup}}] + 2 \times [\text{CO}_{2\,\text{Cat}} - \text{CO}_{2\,\text{Sup}}].$$

Values of Q obtained for the different catalysts after their air pretreatments are compiled in Table 4 and show that the dispersion of tungsten oxide decreases in the order HW > HWe > HWa. These results are consistent with those obtained with HRTEM. Furthermore, the greatest dispersion was obtained after pretreatment of the catalysts in dry air, because the presence of humidity in the atmosphere of the treatment favors the sintering of the metal oxide phase, as commented above.

The distribution and chemical nature of the metal oxide phase were studied by XPS. The spectra of O_{1S} and W_{4f} levels for catalyst HW pretreated in wet air are depicted, as examples, in Figs. 5 and 6, respectively. The O_{1S} core-level spectra of the supported catalysts showed two components: a peak at around 532.0 eV, assigned to C=O bonds from the support in ketones and carboxylic acids [43], and also to W–O bonds [3,44,45]; and a peak at around 533 eV, assigned to oxygen bonded to the support [43].

The measured binding energies (BEs) of $W_{4f_{7/2}}$ were between 35.5 and 36.1 eV (Table 5). These values are characteristic of tungsten (VI) surrounded by oxide ions. Catalyst HW had a lower BE (up to 0.5 eV) than catalyst HWa after air pretreatments. This may be related to the greater dispersion of the former catalyst, which can create possible metal oxide–support interactions through the terminal oxygen of the metal oxide nanocrystals and the oxygen surface complexes of the support. Similarly to the distorsion found in the environment of tungsten oxide deposited on SiO_2 [27], ZrO_2 [46], TiO_2 [47], and Al_2O_3 [22].

The ratio between the number of tungsten atoms determined by XPS and the total number of tungsten atoms determined by chemical analysis ($\%W_{\text{XPS}}/\%W_{\text{Total}}$) was calculated, and the results obtained are depicted in Fig. 7. This parameter can give an idea of the uniformity of the metal oxide distribution. It decreased in the order HWe > HWa > HW, reflecting the decrease of the tungsten oxide concentration on the more external surface of the carbon particles. Thus, for the HW catalyst the tungsten oxide would be more uniformly distributed on the pore network of the support This is derived from its method of preparation, by sublimation.

Many catalytic reactions have been used to quantify the surface acidity of catalysts [48]. Ai and co-workers [49–54] proposed the decomposition reaction of isopropanol to indirectly determine the acid-base character. From a mechanistic point of view, the dehydration is catalyzed by acid sites and the dehydrogenation is catalyzed by both acid and base sites.

Table 5
Binding energy values (eV) of the $W4f_{7/2}$ core-level spectra for the catalysts after different pretreatments

Sample	Pretreatment		
	He	Dry air	Wet air
HW	36.1	35.5	35.7
HWa	36.1	36.0	36.0
HWe	–	–	35.9

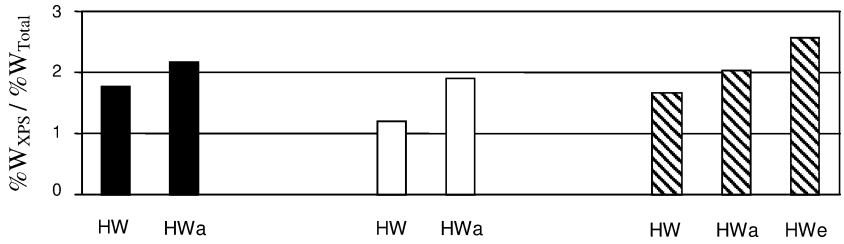

Fig. 7. $\%W_{XPS}/\%W_{Total}$ ratio for catalysts pretreated in He (closed), dry air (open), and wet air (stripes).

Therefore, the rate of dehydration is a measurement of total surface acidity, while the ratio between the rates of dehydrogenation and dehydration is a measurement of the total surface basicity.

Propene and acetone were the only products obtained with all catalysts. The activity to obtain propene, r_p, largely increased with the reaction temperature, whereas there was hardly any change in the activity to obtain acetone, r_a, under the same conditions (Fig. 8). Diisopropylether was detected in all cases but in negligible amounts, and so will not be taken into account in the following discussion. These results indicate that the catalysts were essentially of acidic character.

Table 6 shows the behavior of the catalysts after pretreatments at a reaction temperature of 383 K. These results clearly indicate that the total surface acidity largely depends on the precursor used and the atmosphere of the pretreatment. Thus, the total surface acidity follows the same order found for the variation in the dispersion of the tungsten oxide, i.e., HW > HWe > HWa.

The variation of the surface acidity of the catalysts with the atmosphere of the pretreatment follows the order wet air > dry air > He. Thus, pretreatment in wet air yields the catalysts with highest surface acidity, because the presence of humidity in the atmosphere creates a larger amount of Brönsted acid sites on the tungsten oxide [55], despite the lower dispersion of catalysts after wet rather than dry air treatment (see above).

Table 6
Results from the decomposition reaction of isopropanol at 383 K: rate for propene formation (r_p) and rate for acetone to propene formation ratio (r_a/r_p)

Catalyst	Pretreatment	r_p (μmol g_w^{-1} min^{-1})	r_a/r_p	E_p (kJ mol^{-1})
HW	He	171.6	0.064	110.1 ± 4.4
HWa	He	24.9	0.179	102.9 ± 6.1
HW	Dry air	785.6	0.041	106.9 ± 7.1
HWa	Dry air	71.7	0.144	103.3 ± 1.2
HW	Wet air	900.8	0.033	105.7 ± 4.7
HWe	Wet air	641.5	0.054	108.2 ± 5.1
HWa	Wet air	134.8	0.120	102.6 ± 2.5

Apparent activation energy for propene formation within the range from 343 to 393 K.

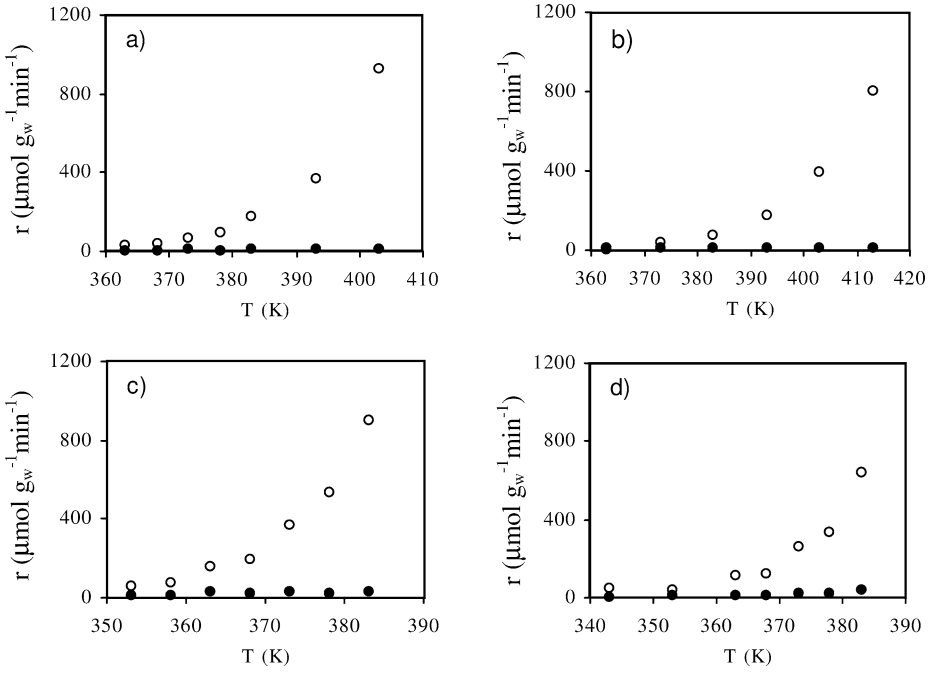

Fig. 8. Rates of propene (○) and acetone (●) formation plotted against reaction temperature in catalysts: HW pretreated in He (a), HWa pretreated in dry air (b), HW pretreated in wet air (c), and HWe pretreated in wet air (d).

Finally, the r_a/r_p ratio was very low and was higher in catalysts with a lower r_p value. Apparent activation energy for propene formation was independent of the type of precursor and pretreatment, which indicates that dehydration follows the same path in all catalysts.

4. Conclusions

The results of our study clearly show the influence of both the type of tungsten precursor and the pretreatment of the tungsten oxide supported on activated carbons on the surface area, metal dispersion and distribution, and total surface acidity of the catalyst. Thus, the surface area of the supported catalysts increased in the order HWe < HWa < HW, and He < dry air < wet air. The dispersion of catalysts obtained by TPD and HRTEM varied in the order HW > HWe > HWa and dry air > wet air > He. Our findings indicate that tungsten oxide particles are formed by very thin sheets or films with very low crystallinity, especially in HW after any of the pretreatments. Dry air produced catalysts with higher dispersion compared with wet air pretreatment, because the presence of humidity sinters the metal oxide particles. Information from XPS indicates that catalyst HW has the most homogeneous distribution of the active phase. In addition, the air treatment of this catalyst seems to create metal oxide–support interactions through the terminal oxygen of the metal oxide nanocrystals and the oxygen surface complexes of the support. Finally, the total surface acidity varied in the order HW > HWe > HWa, the same order as for the metal oxide dispersion. The variation with the pretreatment atmosphere was wet air > dry air > He. Thus, although wet air produced lower dispersion than dry air, it produced a higher surface acidity because the presence of humidity created more Brönsted-type acid centers, which are the active sites for the dehydration of isopropanol.

Acknowledgment

The research described in this work was supported by DGESIC, Project No. PB97-0831.

References

[1] K.T. Ng, D.M. Hercules, J. Phys. Chem. 80 (1976) 2094.
[2] F.P. Kerkhof, J.A. Moulijn, A. Heeres, J. Electron Spectrosc. Relat. Phenom. 14 (1978) 453.
[3] L. Salvati Jr., L.E. Makovsky, J.M. Stencel, F.R. Brown, D.M. Hercules, J. Phys. Chem. 85 (1981) 3700.
[4] L.L. Murrell, D.C. Grenoble, R.T.K. Baker, E.B. Prestidge, S.C. Fung, R. Chianelli, S.P. Cramer, J. Catal. 79 (1983) 203.
[5] S.S. Chan, I.E. Wachs, L.L. Murrell, L. Wang, W.K. Hall, J. Phys. Chem. 88 (1984) 5831.
[6] J.A. Horsley, I.E. Wachs, J.M. Brown, G.H. Via, F.D. Hardcastle, J. Phys. Chem. 91 (1987) 4014.
[7] D.C. Vermaire, P.C. Van Berge, J. Catal. 116 (1989) 309.
[8] M. Wojciechowska, W. Gut, V. Szymenderska, Catal. Lett. 7 (1990) 431.
[9] R.L. Brady, D. Southmayd, C. Contescu, R. Zhang, J.A. Schwarz, J. Catal. 129 (1991) 195.
[10] M.A. Vuurman, I.E. Wachs, J. Phys. Chem. 95 (1991) 9928.
[11] F. Hilbrig, H.E. Göbel, H. Knözinger, H. Schmelz, B. Lengeler, J. Phys. Chem. 95 (1991) 6973.
[12] G. Ramis, G. Busca, C. Cristiani, L. Lietti, P. Forzatti, F. Bregani, Langmuir 8 (1992) 1744.
[13] M.A. Vuurman, I.E. Wachs, J. Phys. Chem. 96 (1992) 5008.
[14] R.B. Quincy, M. Houalla, D.M. Hercules, J. Anal. Chem. 346 (1993) 676.
[15] F.M. Mulcahy, M. Houalla, D.M. Hercules, J. Catal. 139 (1993) 72.
[16] S. Colque, E. Payen, P. Grange, J. Mater. Chem. 4 (1994) 1343.
[17] L. Pizzio, C. Cáceres, M. Blanco, Catal. Lett. 33 (1995) 175.
[18] I. Rodríguez-Ramos, A. Guerrero-Ruiz, N. Homs, P. Ramírez de la Piscina, J.L.G. Fierro, J. Mol. Catal. A 95 (1995) 147.
[19] G. Marci, L. Palmisano, A. Sclafani, A.M. Venezia, R. Campostrini, G. Carturan, C. Martin, V. Rives, G. Solana, J. Chem. Soc., Faraday Trans. 92 (1996) 819.
[20] D.S. Kim, M. Ostromecki, I.E. Wachs, J. Mol. Catal. A: Chem. 106 (1996) 93.
[21] I.E. Wachs, Catal. Today 27 (1996) 437.
[22] L. Karakonstantis, H. Matralis, Ch. Kordulis, A. Lycourghiotis, J. Catal. 162 (1996) 306.
[23] J. Engweiler, J. Harf, A. Baiker, J. Catal. 159 (1996) 259.
[24] J. Ramírez, A. Gutiérrez-Alejandre, J. Catal. 170 (1997) 108.
[25] V.M. Benitez, C.A. Querini, N.S. Fígoli, R.A. Comelli, Appl. Catal. A 178 (1999) 205.
[26] V. Logie, G. Maire, D. Michel, J.-L. Vignes, J. Catal. 188 (1999) 90.
[27] X. Xia, R. Jin, Y. He, J. Deng, H. Li, Appl. Surf. Sci. 165 (2000) 255.
[28] Z.R. Yue, W. Jiang, L. Wang, S.D. Gardner, C.U. Pittman, Carbon 37 (1999) 1785.
[29] C. Moreno-Castilla, F.J. Maldonado-Hódar, J. Rivera-Utrilla, E. Rodríguez-Castellón, Appl. Catal. A 183 (1999) 345.
[30] M.A. Alvarez-Merino, F. Carrasco-Marín, J.L.G. Fierro, C. Moreno-Castilla, J. Catal. 192 (2000) 363.
[31] M.A. Alvarez-Merino, F. Carrasco-Marín, C. Moreno-Castilla, J. Catal. 192 (2000) 374.
[32] C. Moreno-Castilla, M.A. Alvarez-Merino, F. Carrasco-Marín, React. Kinet. Catal. Lett. 71 (2000) 137.
[33] B. Pawelec, R. Mariscal, J.L.G. Fierro, A. Greenwood, P.T. Vasudevan, Appl. Catal. A 206 (2001) 295.
[34] C. Moreno-Castilla, M.A. Alvarez-Merino, F. Carrasco-Marín, J.L.G. Fierro, Langmuir 17 (2001) 1752.
[35] L.R. Radovic, F. Rodríguez-Reinoso, in: P.A. Thrower, M. Dekker (Eds.), Chemistry and Physics of Carbon, Vol. 25, Dekker, New York, 1997, p. 243.
[36] M.V. López-Ramón, C. Moreno-Castilla, J. Rivera-Utrilla, R. Hidalgo-Álvarez, Carbon 31 (1993) 815.
[37] C. Moreno-Castilla, M.A. Salas-Peregrín, F.J. López-Garzón, J. Mol. Catal. A: Chem. 95 (1995) 223.
[38] C. Moreno-Castilla, M.A. Salas-Peregrín, F.J. López-Garzón, Fuel 74 (1995) 830.
[39] R.C. Bansal, J.B. Donnet, F. Stoeckli, Active Carbon, Dekker, New York, 1988.
[40] C. Moreno-Castilla, F. Carrasco-Marín, C. Parejo-Pérez, M.V. López-Ramón, Carbon 39 (2001) 869.
[41] M. Inagaki, New Carbons. Control of Structure and Functions, Elsevier, Amsterdam, 2000.
[42] O. Kubachewski, E.L. Evans, C.R. Alcock, Metallurgical Thermochemistry, Pergamon, New York, 1967.
[43] E. Desimoni, G.I. Casella, A.M. Salvi, Carbon 30 (1992) 521.
[44] F. Verpoort, L. Fiermans, A.R. Bossuyt, L. Verdonck, J. Mol. Catal. A 90 (1994) 43.
[45] C.D. Wagner, W.M. Riggs, L.E. Davis, J.F. Moulder, G.E. Muilenberg (Eds.), Handbook of X-Ray Photoelectron Spectroscopy, Perkin–Elmer, Physical Electronics Division, Eden Prairie, MI, 1978.

[46] J.R. Sohn, M.Y. Park, Langmuir 14 (1998) 6140.
[47] A. Scholz, B. Schnyder, A. WoKaun, J. Mol. Catal. A 138 (1999) 249.
[48] A. Gervasini, A. Auroux, J. Catal. 131 (1991) 190.
[49] M. Ai, S. Suzuki, J. Catal. 30 (1973) 362.
[50] M. Ai, T. Ikawa, J. Catal. 40 (1975) 203.
[51] M. Ai, J. Catal. 40 (1975) 327.
[52] M. Ai, J. Catal. 40 (1975) 318.
[53] M. Ai, Bull. Chem. Soc. Jpn. 49 (1976) 1328.
[54] M. Ai, Bull. Chem. Soc. Jpn. 50 (1977) 2579.
[55] G. Busca, Phys. Chem. Chem. Phys. 1 (1999) 723.